LBL-28759

Lawrence Berkeley Laboratory
UNIVERSITY OF CALIFORNIA

EARTH SCIENCES DIVISION

To be presented at the International Conference on Rock Joints, Loen, Norway, June 4–6, 1990, and to be published in the Proceedings

Hydrological Characterization of Variable-Aperture Fractures

Y.W. Tsang and C.F. Tsang

January 1990

Prepared for the U.S. Department of Energy under Contract Number DE-AC03-76SF00098.

LBL--28759

DE90 011603

Hydrological Characterization of Variable-Aperture Fractures

Y. W. Tsang and C. F. Tsang

Earth Sciences Division
Lawrence Berkeley Laboratory
University of California
Berkeley, California 94720

January 1990

This work was supported by the Director, Office of Energy Research, Office of Basic Energy Sciences, Engineering and Geosciences Division, and by the Director, Office of Civilian Radioactive Waste Management, Office of Facilities Siting and Development, Siting and Facilities Technology Division, of the U.S. Department of Energy under Contract No. DE-AC03-76SF00098.

Hydrological Characterization of Variable-Aperture Fractures

Y. W. Tsang and C. F. Tsang
Earth Sciences Division
Lawrence Berkeley Laboratory
Berkeley, California 94720
U. S. A.

ABSTRACT: We have chosen a statistical description of a fracture with variable apertures by means of three parameters, two related to the aperture distribution: the mean aperture b, and the standard deviation σ_b, and one to the spatial arrangement of the apertures, the spatial correlation length λ. Starting with a mathematical description of the geometry of the void space of real fractures, we use geostatistical method to generate a large number of realizations of these mathematical fractures, perform numerical flow and transport experiments on them with particular emphasis to correlate the fracture geometry parameters with observed measurable hydrological quantities. Based on these theoretical studies, we suggest methods to determine the basic parameters which characterize the fractures by means of flow measurements and tracer breakthrough curves. We advocate the need for this kind of hydrological measurements and interpretation, being more direct than geophysical measurements where the correspondence between observations and hydrological properties is still ambiguous. Currently we are applying our proposed methods to various laboratory and field data to test their validity and usefulness.

1 INTRODUCTION

The simplest idealization of a rock fracture is a pair of parallel plates separated by a constant separation (aperture). In this approximation, the volumetric flow through the fracture varies as the cube of the aperture. This simple flow and aperture relationship begins to break down as rough-walled fractures under stress deviate from the parallel-plate idealization (Witherspoon et al. 1980). In the past decade researchers have employed more realistic description of a rock joint with a range of apertures and the impact of the aperture variation within a single rock joint on its flow properties has been recognized (e.g. Tsang and Witherspoon, 1981, Tsang 1984, Gentier 1986, Brown 1987). Detailed measurements of fracture apertures have been obtained by joint surface profiling (Bandis et al. 1981, Brown and Scholz 1985, Gentier 1986), low melting-point metal injection (Pyrak-Nolte et al. 1987, Gale 1987), and resin casting technique (Hakami 1988, Gentier et al. 1989). These measurements have provided useful and important data for the basic studies of flow and transport through variable-aperture fractures. However, in practical field problems it is neither feasible nor practical to make such detailed measurements of apertures in all fractures participating in the flow and transport. Furthermore, aperture measurements of exposed fractures at the borehole walls, tunnel walls or core samples may be affected by the drilling or evacuation process so that they may not be representative of the fractures in the rock mass.

Alternate methods to characterize the apertures are needed. These methods should be hydrological if one is interested in flow and transport properties of the rock since it may not be possible to correlate geophysical results and flow properties simply. Our approach is to study in detail the relationship between certain flow and transport measurements of variable-aperture fractures, and to design hydrological methods to obtain these aperture parameters. In this paper, we shall start with a mathematical description of the geometry of the void space of real fractures, use geostatistical method to generate a large number of realizations of these fractures, perform numerical flow and transport experiments on them. From the insight gained from these numerical experiments on the relationship of the fracture void geometry and hydrological properties,

we design hydraulic measurements to get an estimation of the geometrical parameters which characterize the rock fractures.

2 MATHEMATICAL DEFINITION OF A VARIABLE - APERTURE FRACTURE

We use an aperture density distribution to represent the range of aperture values in a single fracture. That the aperture values of laboratory core samples usually follow a skewed distribution well approximated by a lognormal distribution has been shown by a number of researchers (Gentier 1986, Gale 1987, Hakami, 1988). The lognormal distribution of apertures b for $b \geq 0$ is given by:

$$n(b)\,db = \frac{1}{\sqrt{2\pi\sigma^2}} \exp\left[\frac{-(\log b - \log b_o)^2}{2\sigma^2}\right] \frac{1}{(\ln 10)\, b}\, db \qquad (1)$$

and defined by two parameters: the mean, $(\log b_o)$, and the standard deviation, σ of the logarithm of the apertures. Note that (1/b) db is the differential of ln b; the normalization factor (ln 10)=2.30258... arises from the definition of the aperture distribution on the base 10 logarithm space. The quantity b_o is the most probable aperture value and is smaller than the mean aperture $\bar{b}$ given by:

$$\bar{b} = b_o \exp((\sigma \ln 10)^2/2). \qquad (2)$$

The variance of the apertures, σ_b^2 is related to the variance of log apertures σ^2 by,

$$\sigma_b^2 = \bar{b}^2 (e^{(\ln 10\,\sigma)^2} - 1). \qquad (3)$$

Three distributions with the same mean aperture $\bar{b} = 80\,\mu m$ but different σ are shown in Figure 1.

Given the aperture probability density distribution of Equation 1, plus a spatial correlation length parameter, λ, a two dimensional field of spatially correlated apertures may be generated by geostatistical methods (for details please see our previous work, Moreno et al. 1988). Many possible spatial distributions or realizations of fracture corresponding to the same value of b_o, σ, and λ may be generated. Figure 2 shows two discretized versions of the fractures so generated. The square region of linear dimension L=1 represent a single fracture which is discretized into square elements to which different aperture values are assigned. The magnitudes of the apertures are indicated by shading, with lighter shading corresponding to larger apertures. Figures 2a and 2b are based on the same input parameters for the lognormal distribution but different correlation lengths of 0.1 L and 0.4 L

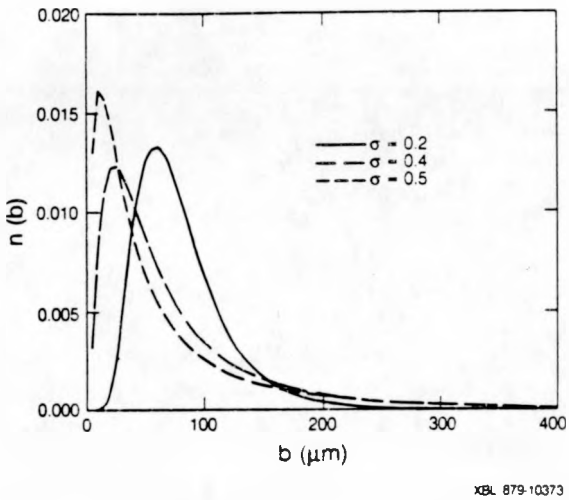

Figure 1 Lognormal distributions with $\bar{b} = 80\,\mu m$, σ = 0.2, 0.4 and 0.5.

respectively. That the apertures are correlated over a longer range in Figure 2b is visually evident.

Thus the variable-aperture fracture is defined in a statistical sense by Equation (1) and the spatial correlation length. The characterization parameters are b_o, σ, and λ. In this way we have avoided the need for detailed deterministic values of apertures b(x,y) at every point in the fractures, which are impossible to determine in-situ. In what follows we describe our studies of how these three basic parameters are correlated to flow and transport and propose ways to estimate these parameters from flow and transport measurements.

3 NUMERICAL FLOW AND TRANSPORT EXPERIMENTS

Given schematic representations of fractures as shown in Figure 2, numerical flow experiments as described in our earlier work (Moreno et al. 1988) may be carried out. The numerical calculations are performed by first discretizing the fracture plane into a 2-D square mesh, each mesh element is assigned a constant aperture. Darcy's law is assumed to apply locally in each mesh element so that the local permeability is proportional to the square of the local aperture. If constant pressures P_1 and P_2 are applied on two opposite boundaries of the square fracture while maintaining no-flow conditions on the remaining two boundaries, the fluid pressure at different points of the fracture can be calculated by solving a matrix equation. From the fluid pressures the local flowrates at different points of the fracture are obtained.

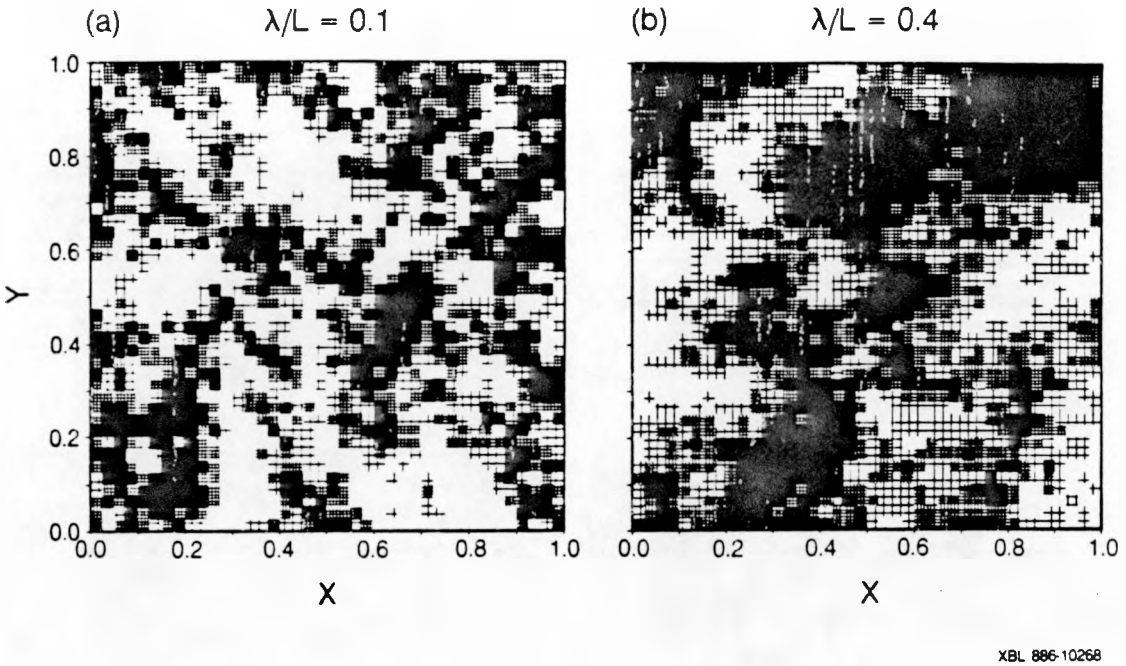

Figure 2 Statistically generated apertures with the same lognormal distribution parameters but different correlation length λ.

Because of the spatial variability of the aperture, the local resistance to flow varies from point to point within the fracture and the flow becomes very non-uniform as σ increases. Figure 3 shows the variation of the local flowrate in a fracture plane. It shows the results for four representations of fracture with the same $\bar{b}$ and λ but different values of σ. Note that the preference of water flowing through paths of least resistance gives rise to the channeling phenomenon, and that the larger the value of the standard deviation in the lognormal aperture distribution σ, the more prominent is the channeling phenomenon.

In addition to the local flowrates, the total steady state flowrate through the fracture from one boundary line to the other may also be obtained. The equivalent permeability of the fracture k for the specified flow geometry is then given by the total flowrate from one boundary line to the other divided by the pressure difference across the fracture. Calculations using many realizations have shown that k is defined within a factor of two for specified b_o, σ, and λ, and it is insensitive to λ if λ is less than 20 to 30% of the size of the flow region. This k is well approximated by the geometrical mean of all the local permeability values. This result is consistent with previous work (Gutjahr et al. 1978, Dagan 1979, Smith and Freeze 1979).

After the steady state fluid flowrates are obtained, the solute transport through the fracture is calculated using a particle tracking method (Moreno et al. 1988). A large number of particles are introduced in the known flow field at one boundary and collected at the opposite boundary of the fracture. When a particle comes to an intersection with two or three outgoing flow sections, a Monte Carlo method is used to assign the particle to one of the flow directions with probability weighted by their respective flowrates. The residence time of the particle in each mesh element is determined from the ratio of the element volume divided by the amount of flow that passes through the element. Summing the residence times over the entire path from inlet to outlet gives the total residence time. A plot of the numbers of particle collected at the outlet at different arrival times constitute the breakthrough curve C(t), the variation of the tracer concentration with time. If the fracture were a pair of parallel-plates, all the particles will arrive at the same time and the breakthrough curve will be a step function. In a real fracture with a range of apertures the tracking particles take different paths with different residence times and typically the breakthrough concentration has a fast rise at early times, since the majority of particles take the fast paths because of flow channeling, then there is a long tail

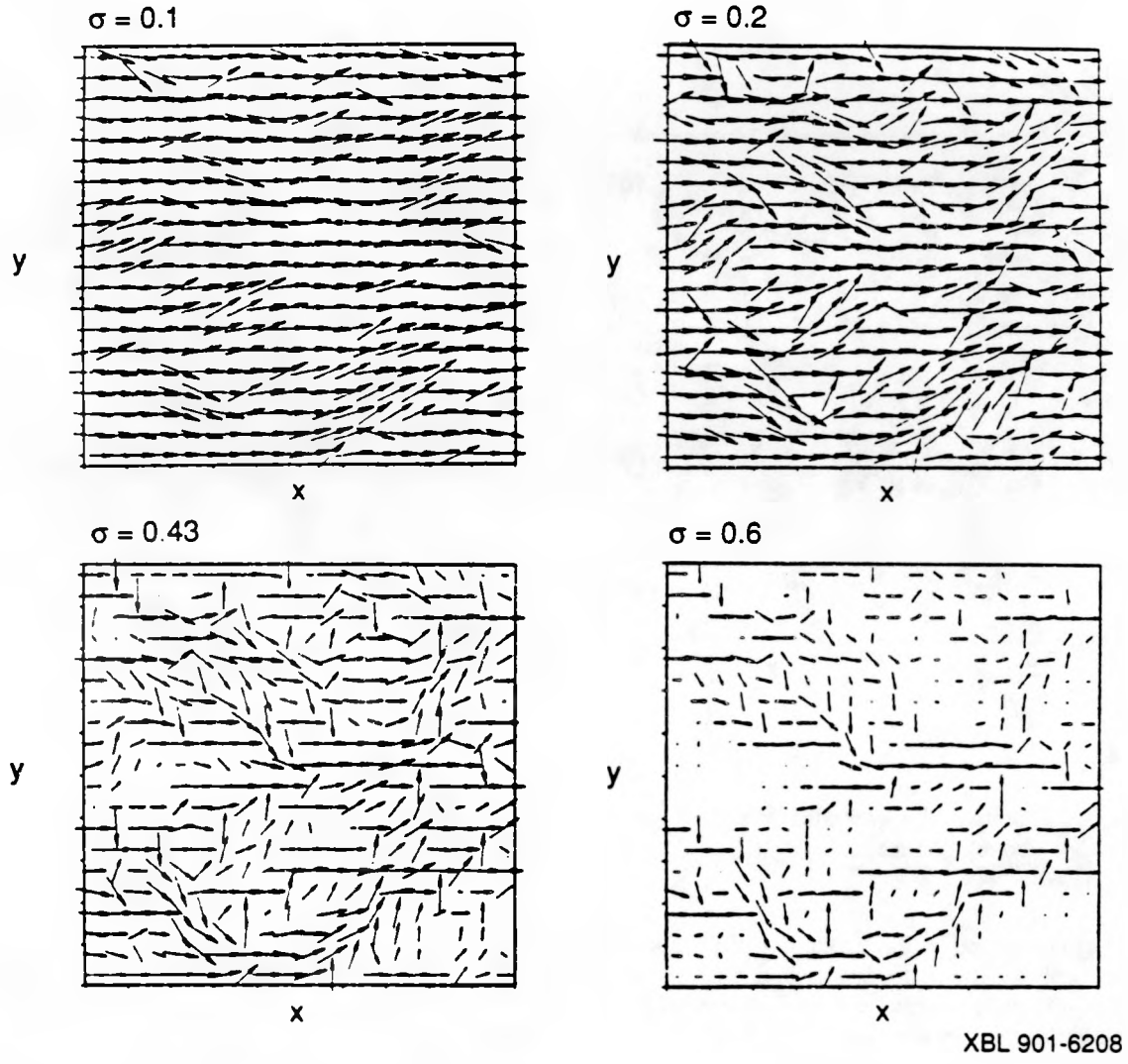

Figure 3 Local flowrates in the plane of a fracture with variable-apertures. Flowrates are proportional to arrow sizes for different values of σ for the same $\bar{b}$ and λ.

in the breakthrough curve due to a small fraction of particles meandering though the fracture, including in their flowpaths many sections with extremely small volumetric flowrates. Figure 4 show examples of breakthrough curves for a step function injection deriving from four realizations of fractures with identical b_o, σ, and λ. In the figure the time axis has been normalized to the mean residence times t_m given by:

$$t_m = \int_0^{\infty} \frac{C(\infty)-C(t)}{C(\infty)}\, dt. \qquad (4)$$

4 DETERMINATION OF MEAN APERTURE FROM FLOW AND TRANSPORT MEASUREMENT

Calculations as described above have been made on a large number of realizations of the variable-aperture fracture. The results point to possible procedures to determine the value of the basic parameters. Table 1 shows the calculated results of tracer residence times for eight different realizations. The mean residence times (t_m) are firstly calculated by particle tracking method as being the mean of the

travel time through the fracture of all the particles (Equation 4). The residence times are also calculated from the ratio of the total fracture void volume and the total flowrate through the fracture Q:

$$t_m = \frac{\bar{b}LW}{Q} = \frac{\bar{b}L^2}{Q,} \qquad (5)$$

where L is the distance between tracer injection and collection, and W is the width of the flow region which equals to L in the representation of square fractures in Figure 2. Table 1 shows that the two ways of calculating mean residence time give values within a few percent, implying that the fracture mean aperture $\bar{b}$ can be estimated hydraulically with Equation 5, using results from two measurements: (1) the total flowrate Q through the fracture, and (2) the mean residence time t_m from tracer breakthrough curves.

It has been a common practice to relate field measurement of flow alone (ratio of flowrate and pressure gradient) to some mean aperture of a fracture. Such flow measurement will gave an erroneous estimate of $\bar{b}$ since it measures an effective permeability of the fracture which we have shown (previous section) is actually the geometric average of the local permeabilities and therefore proportional to b_o^2. For a lognormal distribution, Equations 1 and 2 show that the geometric mean b_o is always smaller than the arithmetic mean $\bar{b}$. The discrepancy between b_o and $\bar{b}$ increases with the spread of the aperture distribution (σ) and can be appreciable.

5 DETERMINATION OF APERTURE VARIANCE FROM TRACER BREAKTHROUGH

To make an estimation of σ, the standard deviation of log apertures in the lognormal distribution (or alternatively σ_b, the standard deviation of apertures), we start with tracer breakthrough curves such as those in Figure 4, which can be measured experimentally. An empirical measure of dispersion may be defined in terms of $(t_{0.9} - t_{0.1})/t_{0.5}$ where t_x is the time when tracer concentration has reached $xC(\infty)$ for a step function tracer injection. This empirical definition of dispersion is directly obtainable from tracer breakthrough curves and is independent of any conceptual model of the medium. Neretnieks et al. (1985) has used this definition and correlated it with the Peclet number in the case of a porous medium. Our simulations

Table 1. Mean residence times calculated from (a) fracture void volume divided by total calculated flowrate, and (b) 2-D particle tracking.

Run	Mean Residence Time (arbitrary units)	
	Fracture Volume/ 2-D Flowrate	Particle Tracking Method
511	0.59	0.59
512	1.46	1.49
513	0.35	0.34
514	0.33	0.33
541	0.07	0.07
542	2.29	2.30
543	0.86	0.85
544	0.30	0.30

have shown that for dispersion in tracer transport, the controlling parameter is σ: the larger the σ, the larger the measure of dispersion $(t_{0.9} - t_{0.1})/t_{0.5}$. The trend of increasing dispersion in tracer breakthrough with larger variance in the fracture aperture variation seems intuitive and is indicated in stochastic theories (e.g. Dagan 1982, 1984; Gelhar and Axness 1983). Figure 3 shows that the local flowrates become increasingly non-uniform as σ increases, implying that for large σ, the spread of

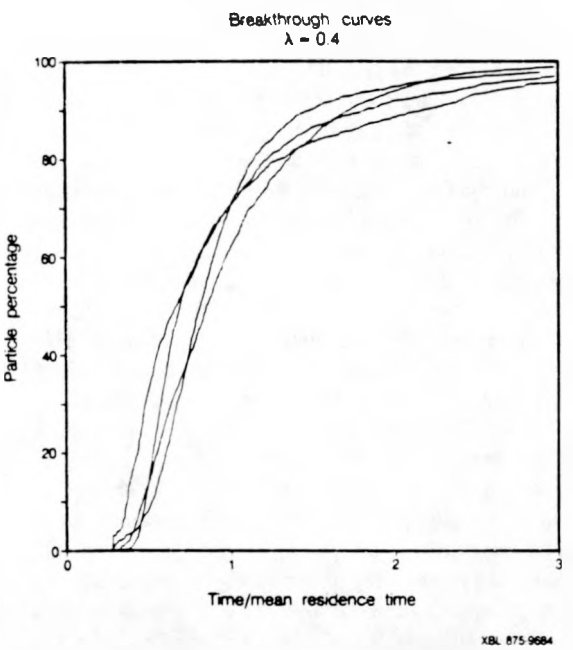

Figure 4 Tracer breakthrough curves from particle tracking.

the residence times of particles tracked through the fracture will increase. We have attempted a systematic study of the dependence of dispersion on channel geometrical parameters by means of a particular theoretical approach which treats fluid flow in 2-D fractures as through a system of statistically equivalent channels (Tsang and Tsang 1987 and Tsang et al. 1988). Our calculations involves (1) numerical simulation in 2-D of flow and tracer transport in a single fracture with variable aperture as described in section 3, (2) determination of the statistics of the aperture values on the particle flow paths, from the 2-D particle tracking simulation, (3) generating by geostatistics method (Tsang and Tsang 1987) 1-D variable-aperture channels which are statistically equivalent, i.e., each channel comprises aperture values consistent with the statistics determined from the previous step, (4) deriving the breakthrough curve from the spread of residence times from such a group of statistically equivalent channels, and (5) plotting of $(t_{0.9}-t_{0.1})/t_{0.5}$ versus the channel parameter $\sigma_b/\bar{b}$.

In Figure 5 we plot the measure of dispersion $(t_{0.9}-t_{0.1})/t_{0.5}$ against the coefficient of variance $S=\sigma_b/\bar{b}$ from the calculational procedure described above. Four different realizations were calculated for each set of S and λ values. We note that the dispersion increases with increasing values of S; and for a fixed S, the dispersion, as well as the spread in dispersion with different statistical realizations, are larger with larger λ values. To get a better handle on the spread of $(t_{0.9}-t_{0.1})/t_{0.5}$ with different statistical realizations, $(t_{0.9}-t_{0.1})/t_{0.5}$ is computed for 80 realizations, all having the aperture parameters S=1.16 and λ/L=0.2. A histogram of their values are shown in Figure 6. The probability distribution of $(t_{0.9}-t_{0.1})/t_{0.5}$ for the 80 realizations has the mean of 2.78, standard deviation of 0.67 and span the range of 1.4 to 4.7. A comparison with Figure 5 shows that the four realizations shown there for the same S=1.16 and λ/L=0.2 span a slightly smaller range, but since the probability distribution in Figure 6 is normal-like, it appears that the values for four realizations in Figure 5 is adequate to bracket the range of possible values of $(t_{0.9}-t_{0.1})/t_{0.5}$. Figure 5 then provides a means to relate the dispersion which can be measured in a tracer transport experiment to the characteristics of the aperture distributions of the flow channels. Thus if a value of $(t_{0.9}-t_{0.1})/t_{0.5}$ is obtained in a tracer experiment, on principle, one can use this figure to estimate the most likely S value of the aperture distribution of the flow channels. Then from the values of S and $\bar{b}$, the value of σ_b or σ for the aperture distribution may be calculated.

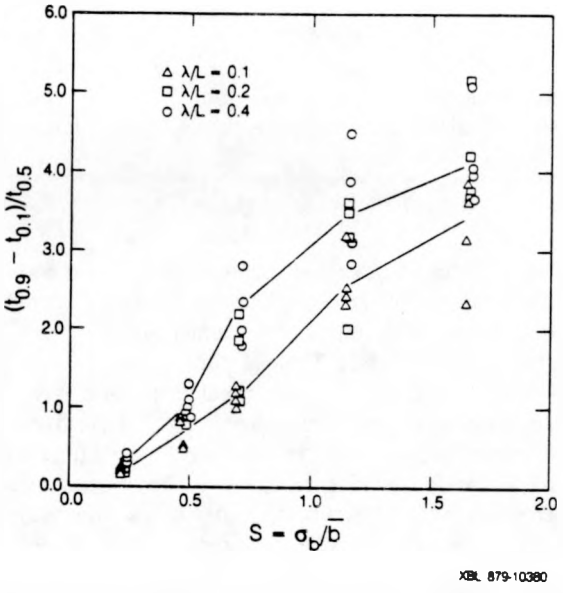

Figure 5 Measure of dispersion versus the coefficient of variance in fracture apertures.

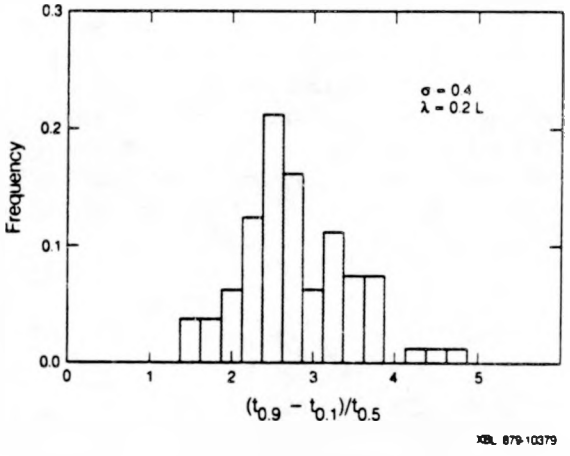

Figure 6 The probability distribution of $(t_{0.9}-t_{0.1})/t_{0.5}$ for 80 realizations with aperture parameter $S=\sigma_b/\bar{b}=1.16$ and λ/L=0.2.

6 DETERMINATION OF APERTURE SPATIAL CORRELATION LENGTH

Previous sections 4 and 5 show that the fracture aperture parameters $\bar{b}$ and σ_b play significant role in fluid flowrate, mean residence time and tracer dispersion, thus allowing their determination from these hydrological measurements. On the other hand, the spatial correlation of the aperture variation hardly affects the above measurable quantities.

In carrying out simulations such as shown in Figure 3 for many relations of the fracture (Moreno et al. 1988, Tsang and Tsang 1989), we found that because of the variation of the apertures within the single fracture plane, the flowrates are very non-uniform, and that there is a tendency for all the flow paths with large flowrates to coalesce into "channels" over a width on the order of one spatial correlation length. The spacing between these large flowrate "channels" is also on the order of the spatial correlation length of the fracture. These results suggest that one may get a rough estimate of spatial correlation length by observing the spatial pattern of the non-uniform flowrates in a line measurement.

In the laboratory, the spatial correlation length of the aperture variation in the fracture may also be deduced from the residual volume of trapped non-wetting phase fluid in an intrusion and withdrawal experiment. Let us consider a fracture with statistically generated apertures such as shown in Figure 2. Assume that the fracture is first evacuated, and then mercury as a non-wetting fluid is intruded simultaneously along four outer edges of the fracture. For intrusion of non-wetting fluid, applied pressure is needed to overcome the capillary pressure, which is given by $P_c = 2\gamma/b$ where γ is the interfacial tension and b is the local aperture. At each pressure P_c, the volume of mercury needed to fill those apertures that have a continuous mercury connection to the four outer edges of the fracture, and are larger than the $b = 2\gamma/P_c$ is calculated. This gives rise to the total capillary curve which is shown in Figure 7 (Tsang and Hale 1988) where on the x axis is the filled volume of mercury V_f normalized to the total available void volume in the fracture V_t. In Figure 7 is also displayed the simulated mercury withdrawal curve from the fracture. As the applied pressure is being released from the final P_c value, the non-wetting mercury in those fracture segments with apertures that are smaller than $2\gamma/P_c$ will spontaneously flow out of the fracture if there exists a continuous path of mercury to the four edges. Since the mercury will stay in place where the apertures are larger than $2\gamma/P_c$, breakage of the continuous mercury phase occur during mercury retraction. As mercury is being expelled from the fracture with the release of external pressure, the smallest aperture will empty first, and mercury in large apertures may become isolated and trapped. If the trapped mercury is predominantly in the large apertures that are isolated by the connected backbone of small apertures, one may expect that the smaller the spatial correlation length of the aperture variation in the fracture, the more opportunity there is for the occurrence of these isolated patches of

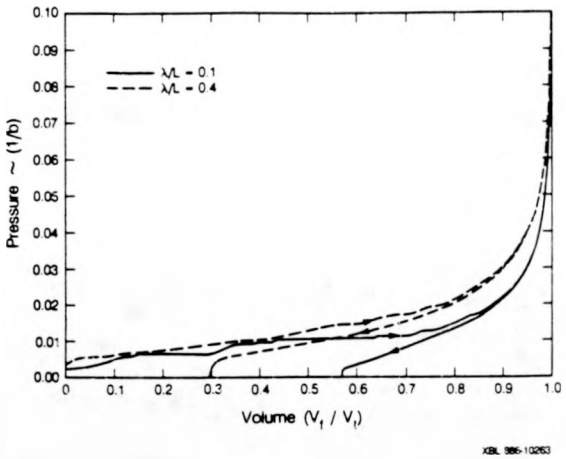

Figure 7 Intrusion and withdrawal capillary pressure curves for the two fracture in Figure 2.

large apertures. One may expect that a larger volume of mercury will be trapped in a fracture with spatial correlation $\lambda/L=0.1$ (Figure 2a) than one with $\lambda/L=0.4$ (Figure 2b). Figure 7 shows the actual simulation of mercury intrusion and withdrawal curves for both fractures in Figure 2. Indeed, the simulation shows that the trapped volume of mercury for the fracture in 2a and 2b are respectively 56% and 30%. Results of a more systematic study are shown in Figure 8 where the residual volume or trapped mercury is plotted against

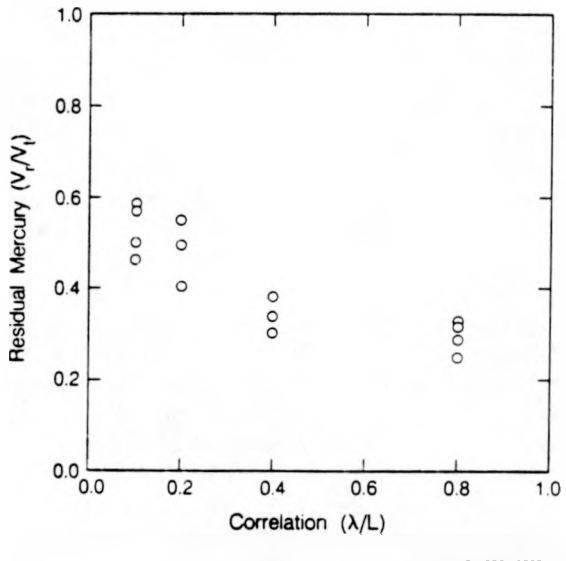

Figure 8 Fraction of trapped residual mercury as a function of spatial correlation length of the aperture spatial variation in the fracture.

the spatial correlation of the aperture variation. Each point corresponds to a simulated result from a different statistical realization of the same fracture aperture distribution. The trend of decreasing trapped mercury with increasing fracture aperture correlation length is apparent. Figure 8 demonstrates that a measure of residual mercury volume in a mercury withdrawal experiment may give useful information on the spatial correlation length of the fracture aperture variation.

7 CONCLUSIONS

A rock fracture with variable apertures cannot be characterized simply by one parameter as in the parallel-plate idealization. We have chosen a statistical description of the fracture by means of three parameters, two related to the aperture distribution: the mean aperture $\bar{b}$, and the standard deviation σ_b, and one to the spatial arrangement of the apertures, the spatial correlation length λ. Based on theoretical and numerical studies, we suggest methods to determine the basic parameters which characterize the fractures by means of flow measurements, tracer breakthrough curves and mercury porosimetry experiments. We advocate the need for this kind of direct hydrological measurements and analyses rather than geophysical measurements where the correlation of observation to hydraulic properties is still ambiguous. Currently we are applying our proposed methods to various laboratory and field data to test their validity and usefulness.

ACKNOWLEDGMENTS

Review and comments from Chalon Carnahan and Joe Wang are gratefully acknowledged. Work is jointly supported by the Director of Office of Energy Research, Office of Basic Energy Sciences, Engineering and Geosciences Division, and by the Director, Office of Civilian Radioactive Waste Management, Office of Facilities Siting and Development, Siting and Facilities Technology Division of the U. S. Department of Energy under Contract No. DE-AC03-76SF00098.

REFERENCES

Bandis, S., Lumisden, A. C. and Barton, N. R. 1981. Experimental studies of scale effects on the shear behavior of rock joints. Int. J. Rock. Mech. Min. Sci., 18: 1-21.

Brown, S. R. and Scholz, C. H. 1985. Broad bandwidth study of the topography of natural rock surfaces. J. Geophys. Res. 90(B14): 12575-12582.

Brown, S. R. 1987. Fluid flow through rock joints: The effect of surface roughness. J. Geophys. Res., 92(B2): 1337-1347.

Dagan, G. 1979. Models of groundwater flow in statistically homoeneous porous formations. Water Resour. Res. 15(1): 47-63.

Dagan G. 1982. Stochastic modeling of groundwater flow by unconditional and conditional probabilities. 2. The solute transport. Water Resour. Res. 18. 835-848.

Dagan G. 1984. Solute transport in heterogeneous porous formations. J. Fluid Mechanics, 145: 151-177.

Gale, J. E. 1987. Comparison of coupled fracture deformation and fluid flow models with direct measurements of fracture pore structure and stress-flow properties. Proceedings of 28th U. S. Symposium of Rock Mechanics, Tuscon, Arizona 29 June-1 July: 1213-1222.

Gelhar, L. W. and Axnes, C. L. 1983. Three-dimensional stochastic analysis of macrodispersion in aquifers. Water Resour. Res. 19(1): 161-180.

Gentier, S. 1986. Morphologie et comportment hydromećanique d'une fracture naturelle dans un granite sous contrainte normale. Doctoral Thesis, U. d'Orleáns, France.

Gentier, S., Billaux, D. and van Vliet, L. 1989. Laboratory testing of the voids of a fracture. Rock Mechanics and Rock Engineering 22: 149-157.

Gutjahr, A. L. Gelhar, L. W., Bakr A. A. and Macmillan, J. R. 1978. Stochastic analysis of spatial variability in subsurface flows, 2, Evaluation and application. Water Resour. Res. 14(5): 953-959.

Hakami, E. 1988. Water flow in single rock joints. Licentiate Thesis, Luleà, University of Technology, Luleà, Sweden.

Moreno, L., Tsang, Y. W., Tsang, C. F., Hale, F. V. and Neretnieks, I. 1988. Flow and tracer transport in a single fracture: A stochastic model and its relation to some field observation. Water Resour. Res. 24(12): 2033-2048.

Neretnieks, I., Eriksen, T. and Tähtinen, P. 1985. Tracer movement in a single fissure in granitic rock: Some experimental results and their interpretation. Water Resour. Res. 18(4): 849-858.

Pyrak-Nolte, L. J., Myer, L. R., Cook, N. G. W. and Witherspoon, P. A. 1987. Hydraulic and Mechanical properties of natural fractures in low permeability rock. Sixth International Congress on Rock Mechanics, Montreal, Canada, 225-231.

Smith, L. and Freeze, R. A. 1979. Stochastic analysis of steady state groundwater flow in a bounded domain 2. two-dimensional simulations. Water Resour. Res. 15(6): 1543-1559.

Tsang, Y. W. and Witherspoon, P. A. 1981. Hydromechanical behavior of a deformable rock fracture subject to normal stress. J. Geophys. Res., 86(B10): 9287-9298.

Tsang, Y. W. 1984. The effect of tortuosity of fluid flow through a single fracture. Water Resour. Res., 20(9): 1209-1215.

Tsang, Y. W. and Tsang, C. F. 1987. Channels model of flow through fractured media. Water Resour. Res., 23(3): 467-479.

Tsang, Y. W., Tsang, C. F., Neretnieks, I. and Moreno, L. 1988. Flow and tracer transport in fractured media: A variable aperture channel model and its properties. Water Resour. Res., 24(12): 2049-2060.

Tsang, Y. W. and Hale, F. V. 1988. A study of the application of mercury porosimetry method to a single fracture. Report LBL-25489, Lawrence Berkeley Laboratory, Berkeley, CA.

Witherspoon, P. A., Wang, J. S. Y., Iwai, K. and Gale, J. E. 1980. Validity of cubic law for fluid flow in a deformable rock fracture. Water Resour. Res., 16(6): 1016-1024.